Supplement of Atmos. Chem. Phys., 20, 10687–10705, 2020
https://doi.org/10.5194/acp-20-10687-2020-supplement

Atmospheric Chemistry and Physics
Open Access
EGU

Supplement of

Trends in eastern China agricultural fire emissions derived from a combination of geostationary (Himawari) and polar (VIIRS) orbiter fire radiative power products

Tianran Zhang et al.

Correspondence to: Tianran Zhang (tianran.zhang@kcl.ac.uk)

Supplement

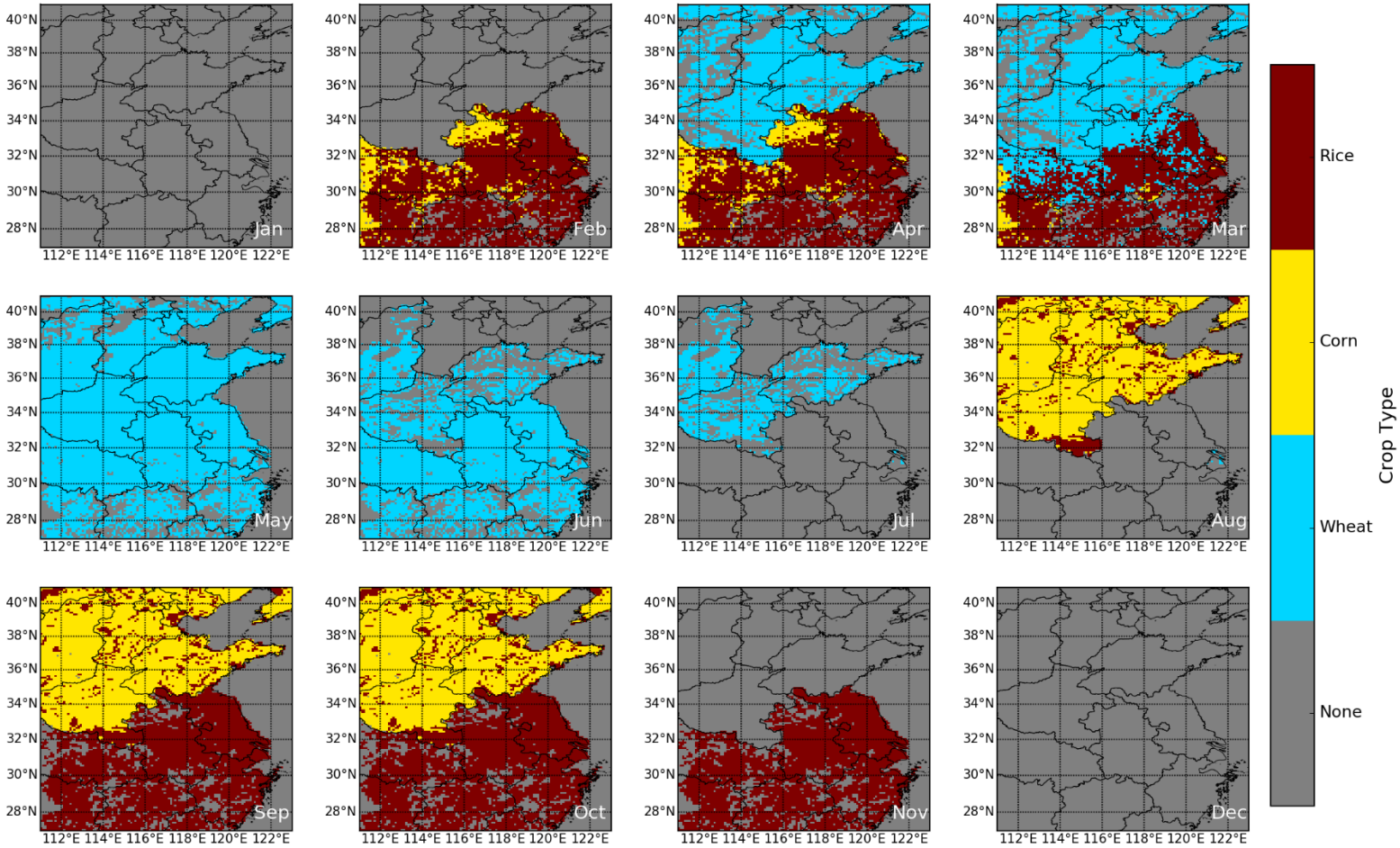

Figure S1: Monthly crop rotation map (0.1×0.1º grid cells) of eastern China generated from the MIRCA2000 rotation cultivation dataset (Portmann et al., 2010).These data were used to both identify the fuel type of each grid cell in which there were fires and to apply the correct emission factor from Table 1. The basic layer of country/province borders within this map was created using Python Basemap librabry.

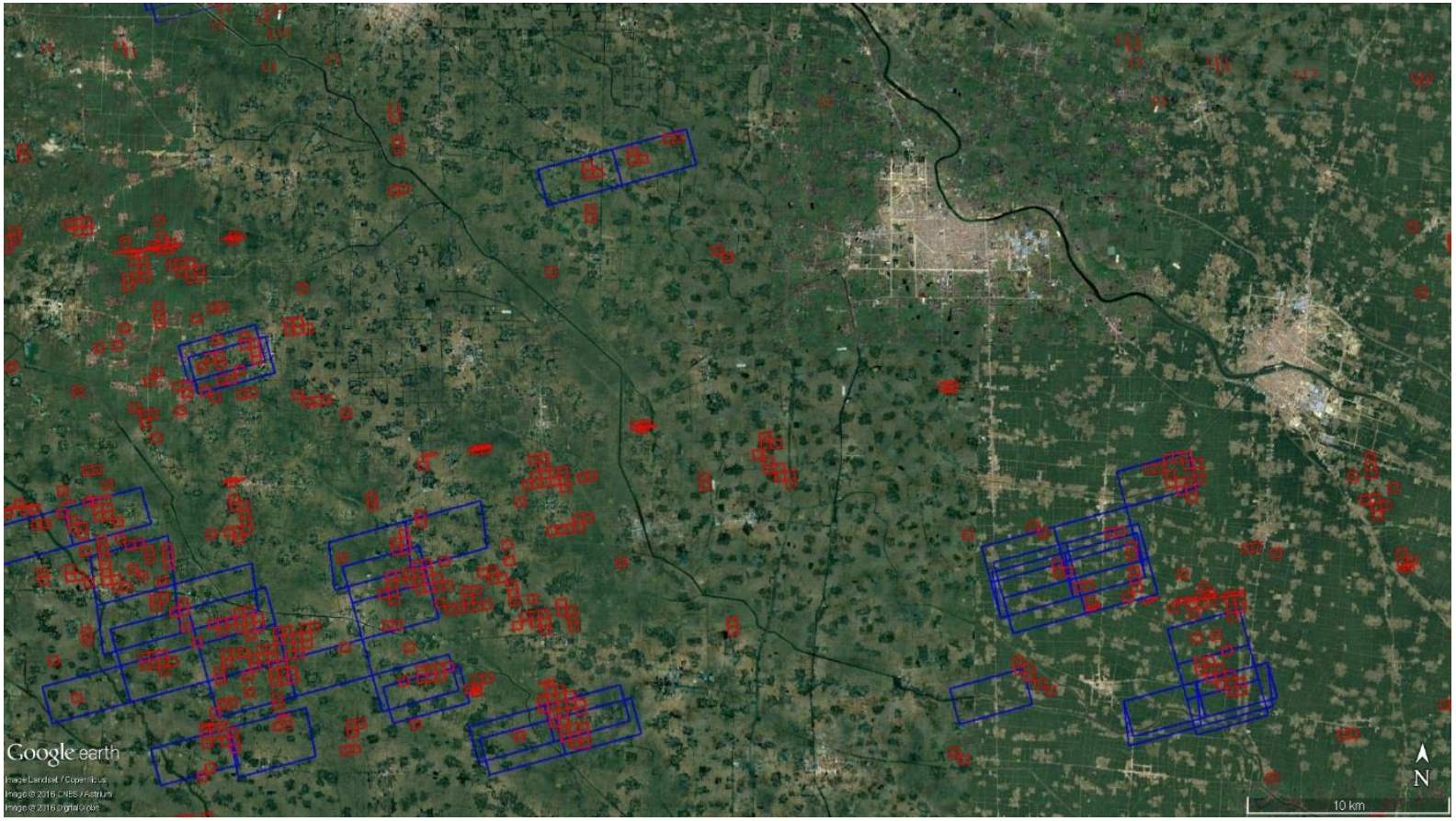

Figure S2: VIIRS (red) and MODIS (blue) fire pixel footprints overlaying Google Earth imagery (June 11th, 2015, © Google Earth). This particular day (11th June) shows unusually high FRP fires for this region, responsible for 62 % of the total VIIRS-IM FRP of the whole of June 2015 (Zhang et al., 2017). The areas of intensive burning area on that day were mainly located towards the edge of swath of for MODIS, but were so large/strongly burning that MODIS could still detect them at these high scan angles. Strong line-to-line duplication of the MODIS pixels shown in this figure have increased the FRP beyond what it would have been were these fires located at nadir, and as a result, likely caused a 1-2x overestimation in MODIS FRP retrieval.

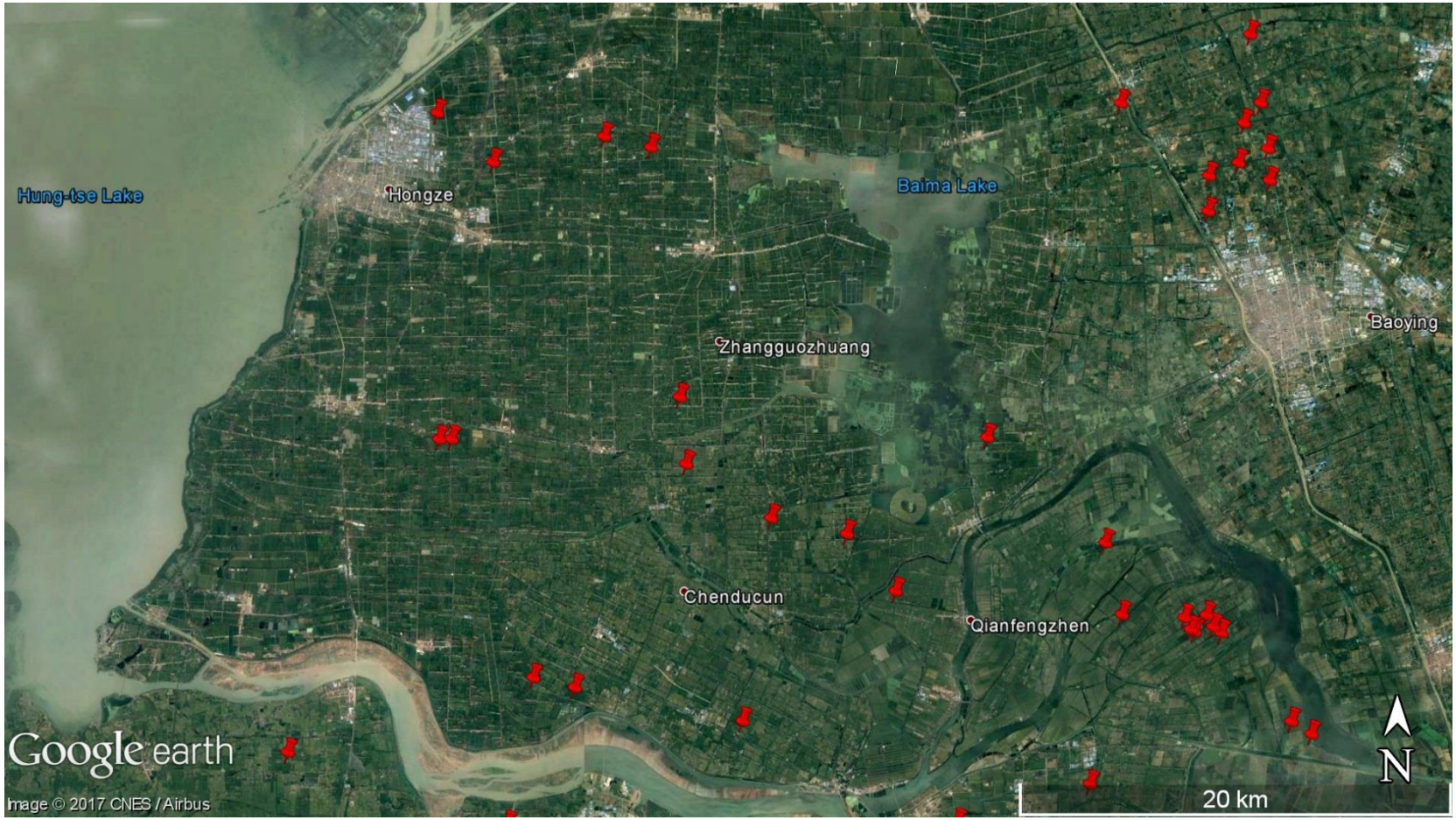

Figure S3: Google Earth imagery (centred at 33.210°N, 119.043°E, © Google Earth) upon which are superimposed the VIIRS active fire pixels (red pin, fire detection algorithm details seen in Section 3.2) from Nov. 20th to Dec. 10th, 2013. The majority of these fire detections are located in agricultural areas, and do not appear to be false alarms (see Section 5.2 for further details)

Figure S4: Evidence for agricultural burning in the winter season (2013). During a live TV news report related to intensive burning of agricultural residues in Hongze, Jiangsu Province (33.2942° N, 118.8731° E) on 5th December 2013, the reporter disappears into the thick smoke (http://www.weibo.com/1301904252/AlVcm8jZ2?type=comment#_rnd1499031542147).

Figure S5. Landsat true colour imagery shows fires over agricultural land on Dec 16th, 2016 near Wuhu City, Anhui (31.429309°N, 117.719021°E). The imagery was taken from USGS/EROS website.

Table S1: Province-specific crop yield of three main grains in Eastern China ($\times 10^1$ Gg, National Bureau of Statistics of China, 2012-2015)

Province	2012			2013			2014			2015		
	Wheat	Corn	Rice	Wheat	Corn	Rice	Wheat	Corn	Rice	Wheat	Corn	Rice
Shanghai	24	3	89	23	3	89	18	3	87	19	3	84
Beijing	28	90	0	27	84	0	19	75	0	12	50	0
Tianjin	54	94	11	56	93	11	57	102	13	59	101	12
Anhui	1216	363	1387	1294	428	1394	1332	426	1362	1394	466	1395
Shandong	2104	1979	104	2180	1995	103	2219	1967	104	2264	1988	101
Shanxi	240	855	1	259	904	1	231	956	1	259	938	1
Jiangsu	1023	226	1864	1049	230	1900	1101	216	1922	1160	239	1912
Jiangxi	2	11	1950	2	13	1976	3	12	2004	3	12	2025
Hebei	1276	1640	60	1338	1650	50	1387	1704	59	1430	1671	54
Henan	3123	1697	475	3177	1748	493	3226	1797	486	3329	1732	529
Zhejiang	27	15	649	27	29	608	28	27	580	31	30	590
Hubei	345	276	1617	371	283	1651	417	271	1677	422	294	1730
Hunan	10	189	2575	9	197	2632	11	185	2562	10	189	2634
Total	9472	7438	10782	9812	7657	10908	10049	7741	10857	10392	7713	11067

Table S2: Proportion of dry matter production-to-residue ratios (R_i) and crop combustion completeness (C, de Zarate *et al.,* 2010; Huang *et al.,* 2012; Turn *et al.,*1997; Wang and Zhang, 2008) from burning of wheat, corn and rice residues. Combustion completeness is high for fine fuels such as these.

	Production-to-residue Ratio	Combustion Completeness
Wheat	1.0	0.86
Corn	2.0	0.92
Rice	1.0	0.89